Journal of Magnetic Resonance 261 (2015) 101–109

Contents lists available at ScienceDirect

Journal of Magnetic Resonance

journal homepage: www.elsevier.com/locate/jmr

Conformational analysis of small organic molecules using NOE and RDC data: A discussion of strychnine and α-methylene-γ-butyrolactone

Andreas Kolmer [a], Luke J. Edwards [b,1], Ilya Kuprov [c], Christina M. Thiele [a,*]

[a] Clemens-Schöpf-Institut für Organische Chemie und Biochemie, Technische Universität Darmstadt, Alarich-Weiss-Strasse 16, 64287 Darmstadt, Germany
[b] Department of Chemistry, University of Oxford, Inorganic Chemistry Laboratory, South Parks Road, Oxford OX1 3QG, United Kingdom
[c] School of Chemistry, Faculty of Natural and Environmental Sciences, University of Southampton, University Road, Southampton SO17 1BJ, United Kingdom

ARTICLE INFO

Article history:
Received 9 April 2015
Revised 2 October 2015
Available online 26 October 2015

Keywords:
Nuclear Overhauser Effect
Residual Dipolar Couplings
Configuration determination
Conformational analysis
Strychnine

ABSTRACT

To understand the properties and/or reactivity of an organic molecule, an understanding of its three-dimensional structure is necessary. Simultaneous determination of configuration and conformation often poses a daunting challenge. Thus, the more information accessible for a given molecule, the better. Additionally to ^3J-couplings, two sources of information, quantitative NOE and more recently also RDCs, are used for conformational analysis by NMR spectroscopy. In this paper, we compare these sources of conformational information in two molecules: the configurationally well-characterized strychnine **1**, and the only recently configurationally and conformationally characterized α-methylene-γ-butyrolactone **2**. We discuss possible sources of error in the measurement and analysis process, and how to exclude them. By this means, we are able to bolster the previously proposed flexibility for these two molecules.

1. Introduction

For the determination of three-dimensional structures of rigid molecules in solution by NMR spectroscopy, usually dihedral angles determined from scalar coupling constants via the Karplus equation [1], distances from the Nuclear Overhauser Effect (NOE) [2–4], and recently the angular information from Residual Dipolar Coupling (RDC) data [5–9] are used.

The structure of flexible molecules is much more difficult to determine. In this case, only averaged NMR parameters are accessible. This complicates structure determination. If one succeeds though, important information about structure and dynamics of the molecule under investigation can be obtained.

Due to the different information content of NOE and RDC and their different behavior under conformational averaging, both interactions might lead to different results. It is difficult to tell in advance whether an approach based on only one kind of parameter will work for a given molecule. In consequence, depending on the molecule, a consideration of only one of the two sets of parameters might thus not be sufficient.

We herein demonstrate a combined NOE/RDC analysis for two molecules, strychnine **1** and α-methylene-γ-butyrolactone **2** (see Fig. 1), and discuss whether a simplified approach would lead to the same results for those molecules.

2. Conformational averaging

When discussing the effects of conformational averaging on the observation of NOE and RDC, first the timescale of the molecular motion has to be identified.

There are two major regimes of conformational flexibility compared to the timescale of chemical shift evolution: slow and fast exchange [10]. In the slow exchange regime, each conformer that

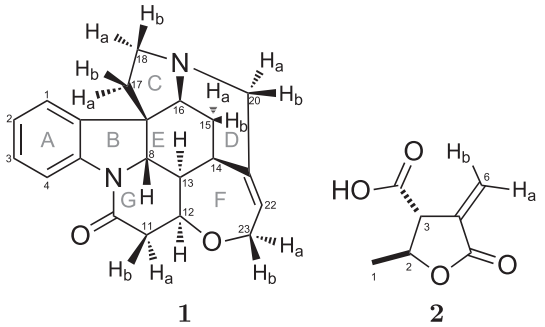

Fig. 1. Chemical structures and nomenclature of strychnine **1** and α-methylene-γ-butyrolactone **2**.

* Corresponding author.
E-mail address: cthiele@thielelab.de (C.M. Thiele).
[1] Current address: Wellcome Trust Centre for Neuroimaging, UCL, 12 Queen Square, London, WC1N 3BG, United Kingdom.

http://dx.doi.org/10.1016/j.jmr.2015.10.007
1090-7807/

is present in solution gives rise to its own set of signals. The number of populated conformers can therefore be identified from the number of signal sets. In the fast exchange regime, the observed signal is an average over all conformers. Thus, a single set of signals is observed, as would be for a rigid compound. From the number of signals, a rigid compound is indistinguishable from a compound undergoing fast conformational exchange.

In the fast exchange regime, there are two different timescales for the motional averaging of NOE derived distances [3]. Compared to the overall tumbling, as characterized by the correlation time τ_C, the conformational flexibility can either be faster than τ_C (slow tumbling) or slower than τ_C (fast tumbling). To avoid confusion, it is necessary to mention that the timescale of the overall tumbling is different from the timescale of chemical shift evolution. Thus we will adopt the terms fast and slow tumbling [3,11] for these two terms, while the terms fast and slow exchange will be applied with respect to the timescale of chemical shift evolution.

If a compound is in the fast tumbling regime [3,11], the observed distance is an average over the individual distances of all populated conformers according to the following Eq. (1) [3]:

$$r_{IS,\text{averaged}} = \left(\sum_{\mu=1}^{N} p_\mu r_{IS,\mu}^{-6}\right)^{-\frac{1}{6}} \tag{1}$$

with N being the number of conformers, p_μ the population of the conformer μ and $r_{IS,\mu}$ the distance of the protons I and S in the conformer μ.

If a compound or a part of a compound is in the slow tumbling regime [3,12,13], the observed distance is an average over the individual distances of all populated conformers according to Tropp [12] and is described by the following Eq. (2):

$$r_{IS,\text{averaged,Tropp}} = \left(\sum_{\mu=1}^{N} p_\mu r_{IS,\mu}^{-3}\right)^{-\frac{1}{3}} \tag{2}$$

For organic compounds, it is difficult to decide which of those two equations needs to be applied. To be certain which equation is the correct one for a given pair of protons, first the overall tumbling rate τ_C needs to be determined. While there are methods to do so (e.g. from ^{13}C relaxation rate constants [3]), usually one single and constant τ_C is assumed for the (organic) compound, which is a problematic assumption in itself. Secondly, the molecular motion needs to be compared to τ_C. This poses a challenge, as the authors are unaware of a way to determine the rate of conformational interconversion in the regime of fast exchange experimentally (if no line broadening due to exchange is present anymore). Thus, it is usually assumed that protons in methyl groups can be described by slow tumbling [3] and are described by Eq. (2) (r^{-3} averaging), while all other protons are assumed to be in the fast tumbling regime [3] and are described by Eq. (1) (r^{-6} averaging).

Averaging of RDC data is a different matter. In anisotropic solution, the overall tumbling is not isotropic and thus cannot be adequately described by the isotropic tumbling rate τ_C. Instead, usually the anisotropic tumbling of a compound is described by the Saupe-tensor S [14] or its scaled analogue, the alignment tensor A [15]. For a rigid compound, one tensor is needed to compare the experimental RDC data to a structural proposal. This is called the single conformer single tensor (SCST) model [9,16–19]. For flexible compounds, ideally one tensor is used for each populated conformer, this is called the multi conformer multi tensor (MCMT) model [9,16–19]. If the conformational interconversion of the compound is fast as compared to the anisotropic tumbling, it might be possible to assume that a single tensor is sufficient to describe the whole ensemble of conformers. This assumption is called the multi conformer single tensor (MCST) model [9,16–19].

It is challenging to judge whether a MCST approach is justified or whether a MCMT approach is necessary. It has been shown for the lactone **2** [19] and for fibrosterol sulfate A [20] that both methods lead to the same result, thus indicating that the assumption of the MCST approach is justified for those two molecules. Its general applicability and its limits are currently under investigation.

3. Strychnine

Strychnine **1** is composed of seven annealed rings and has been considered to be highly rigid. Its rigidity and well-known complex structure led to strychnine **1** being a challenging target molecule for total synthesis [21–23] and to it being used as test molecule for NMR method development [24]. Correspondingly, when a hidden flexibility of strychnine **1** in either ring C [25] or ring F [26,27] was proposed, these results were met with astonishment.

Butts et al. discovered that one distance (H_{11b}–H_{23b}) in a 1D Pulsed Field Gradient Spin Echo (PFGSE) NOE experiment can only be explained by conformational flexibility of ring F in strychnine [26]. This is also in accordance with DFT-calculations performed by the same group, in which 1–2% of the second conformer was proposed based on the free energy difference [26]. The distance H_{11b}–H_{23b} shows the best agreement when adding a second conformer **1f2** with a population of 2.2%. The two conformers **1f1** and **1f2** are shown in Fig. 2.

It should be noted though that Butts et al. did not degas the sample and performed only one (series of) measurement(s) at a single mixing time of 500 ms. This does not allow one to check the validity of the initial-rate approximation [28]. In another paper [11] Butts et al. describe that the initial-rate-approximation is fulfilled for strychnine **1** for up to 600 ms. Another aspect is that at 600 MHz the protons H_{23a} and H_{23b} are strongly coupled (strong coupling parameter [3] $\theta = 0.52$). Although Butts et al. use a zero-quantum suppression (ZQS) element [29–31], full ZQS might not be possible depending on the coupling constant and effectiveness of ZQS [30] and may thus obscure the NOE intensity between H_{11b} and H_{23b}. Finally, the relaxation delay of 1 s should be mentioned, which is too short to assure complete relaxation. Butts et al. assume that the NOE obtained can be quantified in spite of all these assumptions. If this is the case, the method of Butts et al. would possess the great advantage that the measurement time can be drastically reduced by not using a mixing time series and complete relaxation. We therefore aim to exclude these potential sources of error and then compare and discuss the results.

Besides the NOE investigations by Butts et al., a RDC analysis was performed by Schmidt et al. [27]. For this, Schmidt et al. proposes two conformers [27] which show the same structures and flexibility as the ones by Butts et al. From integration of signals

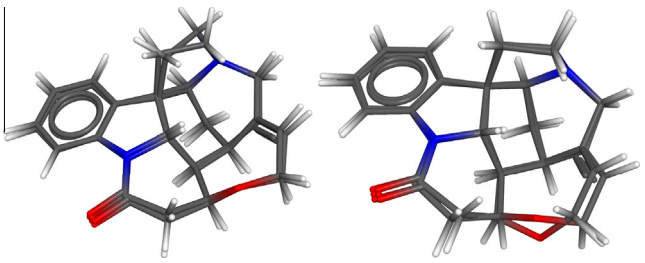

Fig. 2. Visualization of the flexibility of strychnine **1**. Left: Two conformers **1c1** and **1c2** according to Bifulco et al. [25], showing the flexibility in ring C. Right: Two conformers **1f1** and **1f2** according to Butts et al. [26] and Schmidt et al. [27], showing the flexibility in ring F.

at low temperatures (slow exchange regime), they extrapolated a population of 2.7% **1f2** at 298 K. In addition, they compare previously published RDC data [32] to an ensemble of conformers. The best agreement has been found at a population of 13% **1f2**. It is observed that the RDC fit is less sensitive to small population changes. Although newer RDC data exists [33,34], fits of these datasets were not shown. We believe the newer RDC data might also allow interesting insights, and thus aim to expand this picture. Further, we will compare the results to the results from the NOE.

In addition to the flexibility of ring F, there are first indications for a flexibility of ring C. Bifulco et al. discovered that calculated $^1J_{CC}$ values for C_7–C_{17} and C_7–C_{16} change significantly if a second conformer **1c2** with another orientation in ring C is introduced [25]. They concluded that the population of **1c2** is very small (0.11% at 298 K). Schmidt et al. considered this as not reliable [27], and thus no comparison with experimental data aside from $^1J_{CC}$ values has been performed. We therefore aim to use experimental NOE and RDC data to also investigate the proposed flexibility of ring C.

3.1. Flexibility of ring F

We quantified several proton–proton NOE signals of strychnine via mixing time series (50–400 ms) of fully relaxed 1D PFGSE NOE [35–37] spectra with ZQS [29–31]. During the period of validity of the initial-rate-approximation [28], we evaluated those mixing time series using the Peak Amplitude Normalization for Improved Cross-relaxation (PANIC) approach [38]:

$$r_{IS} = r_{\mathrm{ref}} \left(\frac{\sigma_{IS}}{\sigma_{\mathrm{ref}}} \right)^{-\frac{1}{6}} \tag{3}$$

where r_{IS} is the distance between I and S that one wishes to determine, and σ_{IS} is the cross-relaxation rate constant which is equal to the slope of the corresponding PANIC plot [38]. r_{ref} stands for a reference distance with σ_{ref} being the slope of the PANIC plot for the reference distance. As reference distance, we chose H_{15a}–H_{15b} as rigid distance between two diastereotopic protons and set it to 1.760 Å. To compensate for different relaxation rates of sp^3- and sp^2-bound protons, we used the relayed calibration as proposed by Butts et al. [11], and in order to remove the confound of paramagnetic atmospheric oxygen, the samples were degassed; see Supporting Information for details.

The resulting distances mostly are in good agreement with the ones by Butts et al. [26] (see Fig. 3). Up to 400 ms mixing time, the initial-rate approximation is valid for all observed distances (see Supporting Information for details).

After determining the distances, we performed a conformational analysis using the self-written software *WEEDHEAD* (see Supporting Information for details). The populations were varied in 1%-steps. Because only one set of signals is present at 300 K, the conformational flexibility was judged to be in the regime of fast exchange. In addition, no exchange signals were found in the NOE spectra, thus indicating that no slow exchange is present. Averaged distances were calculated using the formula (1) [3], assuming fast tumbling (r^{-6} averaging). The averaged distances can then be compared to the experimental values. For H_{11b}–H_{23b}, this comparison can be found in Fig. 4.

We have been able to determine 33 distances in total (see Supporting Information). All of these distances can be compared to averaged distances. At the correct population of the two conformers **1f1** and **1f2**, the overall agreement between experimental and averaged distances should be best. Therefore, for each population we determine a quality factor q comparable to the one proposed by Cornilescu et al. [39] for anisotropic NMR parameters:

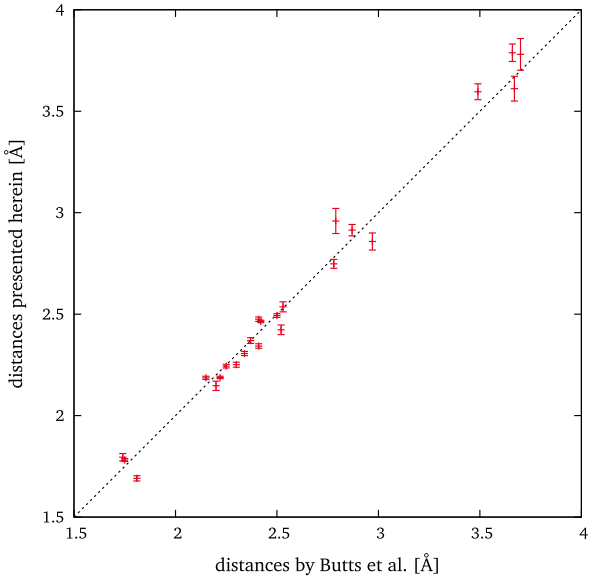

Fig. 3. A comparison of the distances in **1** determined by us (y-axis) from cross-relaxation rates (mixing time series of 50–400 ms of fully relaxed PFGSE NOE spectra with ZQS) and by Butts et al. [26] (x-axis, from PFGSE NOE spectra with ZQS, a relaxation delay of 1 s and a single mixing time of 500 ms).

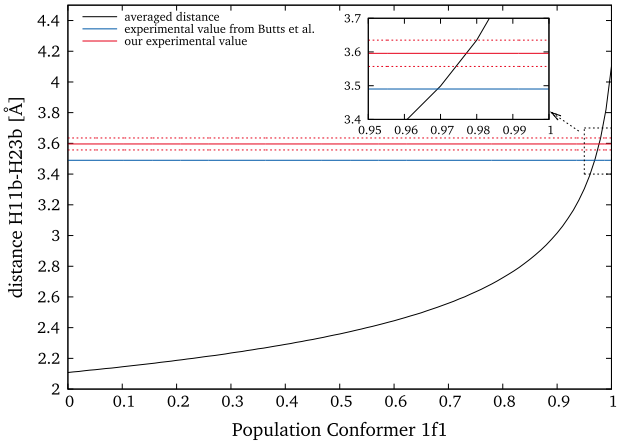

Fig. 4. A comparison of the distance H_{11b}–H_{23b} averaged from **1f1** and **1f2** by Eq. (1) (black) and the experimental values by us (red, experimental error represented as dashed lines) and by Butts et al. [26] (blue). The enlarged section shows a perfect agreement for a population of the conformer A of 98% for our value, or at 97% for Butts et al. (For interpretation of the references to color in this figure legend, the reader is referred to the web version of this article.)

$$q = \frac{\sqrt{\frac{1}{N}\sum_{IS}\left(r_{IS,\mathrm{averaged}} - r_{IS,\mathrm{exp}}\right)^2}}{\sqrt{\frac{1}{N}\sum_{IS}\left(r_{IS,\mathrm{exp}}\right)^2}} \tag{4}$$

(with N the number of distances and $r_{IS,\mathrm{exp}}$ the experimentally determined distance between spin I and spin S) and search for the minimum (see Fig. 5).

Again, our results are in good agreement with the results from Butts et al. [26], and our agreement of the experimental distances with the conformationally averaged distances is even slightly better. The minimum at 98% of **1f1** is essentially the same as determined by the comparison of only H_{11b}–H_{23b} (see Fig. 4). Thus, in this case, the analysis of one distance would be sufficient.

The common school of thought is that CH- and CH_2–groups in small organic molecules are in the fast tumbling regime [3]. For the above analysis, r^{-6} averaging has been performed according

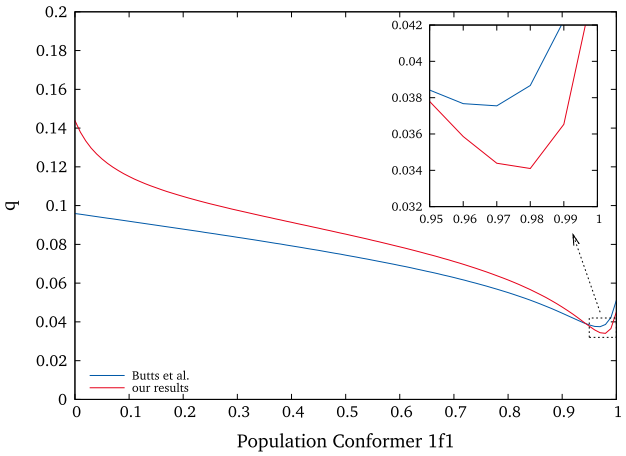

Fig. 5. Conformational analysis of **1** using our distances (red) and the ones from Butts et al. [26] (blue). The y-axis shows the quality factor q (Eq. (4)). The lower the quality factor, the better the agreement of all experimental distances to the distances averaged from conformers **1f1** and **1f2** by Eq. (1). The best agreement can be found at a population of 98% **1f1** for our values, or at 97% for Butts et al. (For interpretation of the references to color in this figure legend, the reader is referred to the web version of this article.)

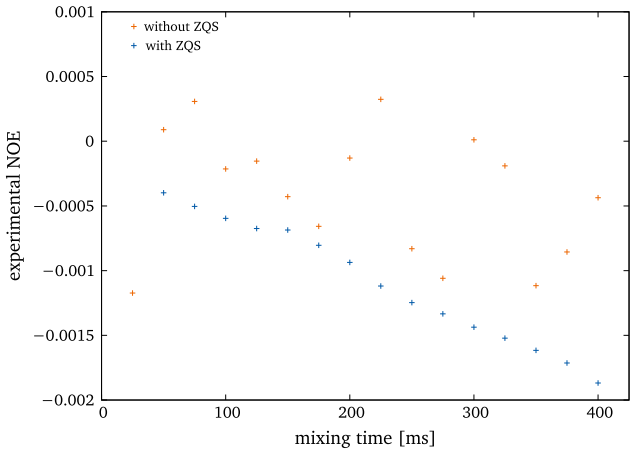

Fig. 6. A comparison of mixing time series for H_{11b}–H_{23b} in **1** with and without ZQS. The modulation can be suppressed quite efficiently by using a ZQS element.

to Eq. (1). However, we also performed an analysis using Eq. (2), which would be correct for slow tumbling (r^{-3} averaging). Surprisingly, the description in fast tumbling (r^{-6} averaging) leads to a description of the experimental data which is just as good as the one for slow tumbling (r^{-3} averaging; see Supporting Information for details on both evaluations).

3.2. Comparison of experimental and simulated NOE for strongly coupled protons

Even though we were able to reproduce the experimental distances from Butts et al. [26], the interpretation of the experimental data needs to be revisited. It might be possible that the presence of a strongly coupled spin system obscures the distance H_{11b}–H_{23b} in a way that no second conformer **1f2** needs to be proposed. Another possible source of error may be spin diffusion. Although it is generally believed that spin diffusion leads to a non-linear behavior of the PANIC plots [3,40], we nevertheless wanted to exclude this possible source of error. This non-linearity might be hidden under a scattering of experimental data points, and thus might have an impact on the extracted distance. The spin diffusion, the strong coupling and the existence of zero-quantum coherences therefore need to be evaluated.

For the distance H_{11b}–H_{23b} itself, the PANIC plots without and with ZQS are shown in Fig. 6. Without ZQS, a modulation is visible. This modulation can be suppressed with the ZQS module, as would be expected (see Fig. 7). Unfortunately, for H_{23b}–H_{11b} the ZQS module fails to suppress this modulation (see Fig. 8). This, again, is in agreement with the expectation. In our 600 MHz spectrometer, the chemical shift difference of the strongly coupled spins H_{23b}–H_{23a} is roughly 50 Hz. Using a swept pulse/gradient pair of 20 ms, this leads to a maximum theoretical suppression of only 16% of the ZQS [29,30]. This leads to obscured intensities of the irradiated signal H_{23b}, which leads to the PANIC plot of H_{23b}–H_{11b} shown in Fig. 8, from which no reliable distance can be extracted.

This behavior can be observed when the irradiated spin is influenced by strong coupling. It cannot be observed when the spin in the strongly coupled system is the observed spin: The corresponding PANIC plot is linear. Still, it cannot be excluded that strong coupling and/or spin diffusion is present. We therefore decided that a full relaxation matrix approach is necessary to exclude those influences.

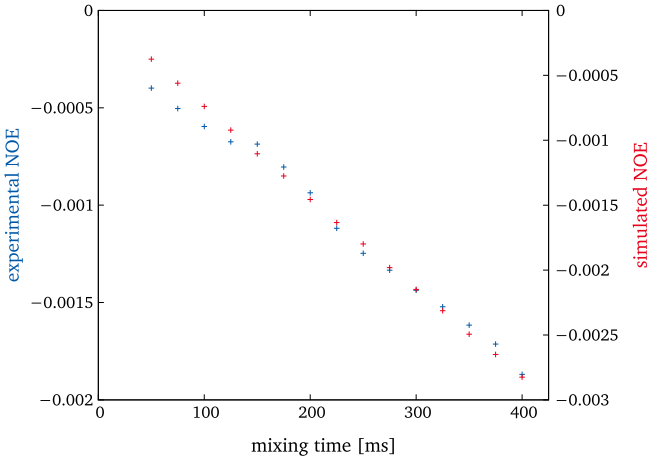

Fig. 7. A comparison of experimental and simulated mixing time series for H_{11b}–H_{23b} in **1** with ZQS. Both the simulated and the experimental PANIC plot show significantly improved linear behavior, thus zero-quantum artifacts are suppressed reasonably well.

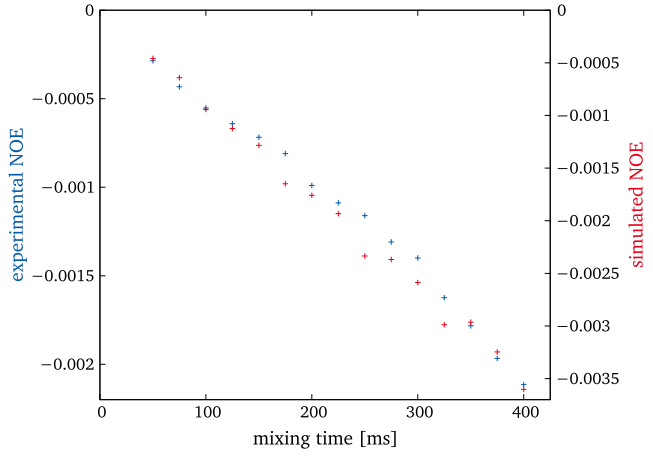

Fig. 8. A comparison of experimental and simulated mixing time series for H_{23b}–H_{11b} in **1** with ZQS. Both the simulated and the experimental PANIC plot show some remaining modulation, thus indicating incomplete ZQS. No reliable distance can be extracted.

Using the *Spinach* library [41–44], we simulated the PANIC plots for the distance H_{11b}–H_{23b}, including the possibility of conformational flexibility (*Spinach* parameters, details of the simulation and the simulated PANIC plots can be found in Supporting Information). The corresponding PANIC plot for a population of 98% **1f1** is shown in Fig. 7, along with the experimental PANIC plot. The conformer populations were varied in 1%-steps between 90% and 100% **1f1**, and in 10%-steps between 0% and 90% **1f1**. Again using H_{15a}–H_{15b} as reference distance, we compared these simulated distances to distances averaged by Eq. (1) (see Fig. 9). The simulated curve corresponds to the expected average distance very well.

This result leads to the conclusion that the main influence on the distance H_{11b}–H_{23b} is conformational flexibility. If strong coupling and/or spin-diffusion obscures the signal intensity, its influence is much weaker and can thus be neglected. It therefore is necessary to add a second conformer to the analysis to be able to explain the experimental distance of H_{11b}–H_{23b}. Thus, the approximations from Butts et al. [26] are valid.

3.3. Flexibility of ring C

It is also possible to compare the determined experimental distances to distances averaged from the structures **1c1** and **1c2** determined by Bifulco et al. [25], which include flexibility at ring C. Of special interest is the distance H_{18b}–H_{20b}, the situation of which is comparable to that of H_{11b}–H_{23b} for ring F: the determined value of (2.343 ± 0.011) Å is slightly too short for conformer **1c1** (2.46 Å). Adding a second conformer **1c2** thus improves the agreement of experimental and averaged distance (see Fig. 10). The single value would lead to a population of 62% **1c1**.

It is again possible to compare all experimental distances to averaged distances, and to determine the quality factor q (Eq. (4)). The result is shown in Fig. 11. In contrast to the previously described situation of ring F, the addition of **1c2** does not improve the quality of the fit, even though the agreement of H_{18b}–H_{20b} improves. On the other hand, the agreement of H_{18a}–H_{20b} and H_{18a}–H_{16} gets worse (data not shown), thus counterbalancing the improvement in H_{18b}–H_{20b}.

A three-conformer-fit including **1f1**, **1f2** and **1c2** was also performed to check for both ring flexibilities in the same fit. Again, no improvement is found when adding **1c2**. The minimum is at 98% **1f1**, 2% **1f2** and 0%**1c2**. The data is shown in Fig. 12.

For ring C, the analysis of one single distance leads to a different result than the analysis of all determined distances and thus needs to be viewed with caution. In this case, it is necessary to look at all distances. As a result, no improvement is achieved when adding a second conformer **1c2**. The main influence on the improvement of the fit is the addition of **1f2**. On the basis of this data, flexibility of ring C can be neglected.

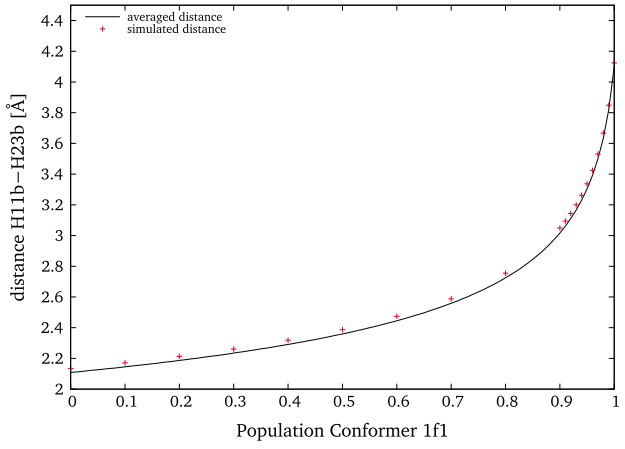

Fig. 9. A comparison of the distance H_{11b}–H_{23b} in **1** simulated with *Spinach* and averaged by *WEEDHEAD*. The very good agreement indicates the necessity of conformational flexibility to explain the experimentally derived distance shown in Fig. 4.

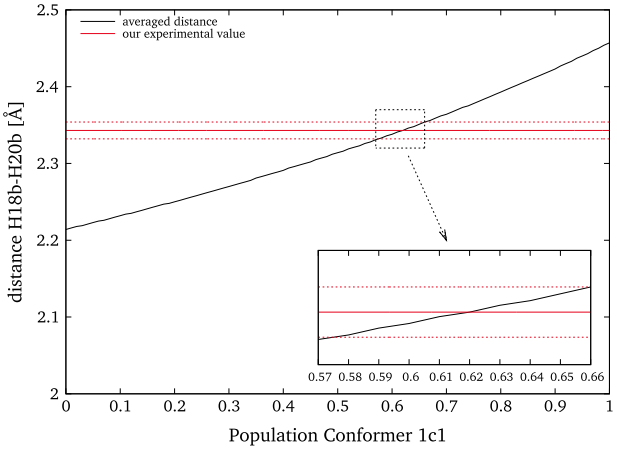

Fig. 10. A comparison of the distance H_{18b}–H_{20b} averaged from conformers **1c1** and **1c2** by Eq. (1) (black) and the experimental value (red, experimental error represented as dashed lines). The enlarged section shows a perfect agreement for a population of 62% **1c1**. (For interpretation of the references to color in this figure legend, the reader is referred to the web version of this article.)

3.4. RDC analysis

Next, we performed a conformational analysis using previously published RDC data. We chose the Multi Conformer Single Tensor (MCST)-method of the program *hotFCHT* [45] (see below), and we will discuss the results based on the quality factor Q as defined by Thiele et al. [19], which includes the experimental error $\Delta D_{i,exp}$ of the i-th experimental RDC $D_{i,exp}$:

$$Q = \frac{\sqrt{\frac{1}{N}\sum_i \left(\frac{D_{i,calc} - D_{i,exp}}{\Delta D_{i,exp}}\right)^2}}{\sqrt{\frac{1}{N}\sum_i \left(\frac{D_{i,exp}}{\Delta D_{i,exp}}\right)^2}} \tag{5}$$

with N being the number of RDCs.

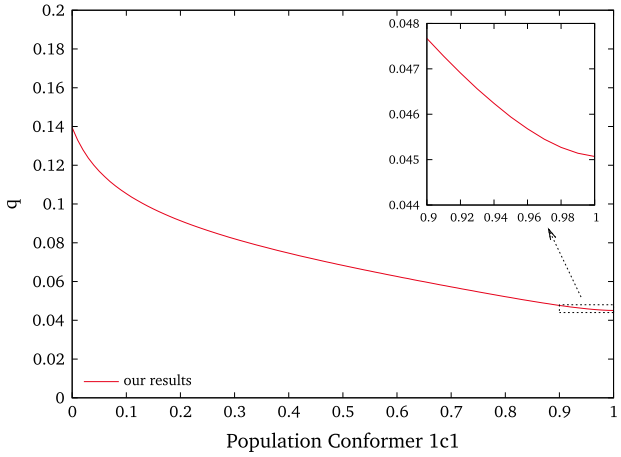

Fig. 11. Conformational analysis of **1** using all our distances (red). The y-axis shows the quality factor q (Eq. (4)). The lower the quality factor, the better the agreement of all experimental distances to the distances averaged from conformers **1c1** and **1c2** by Eq. (1). No improvement can be found when adding **1c2**, the broad minimum lies at 100% **1c1**. (For interpretation of the references to color in this figure legend, the reader is referred to the web version of this article.)

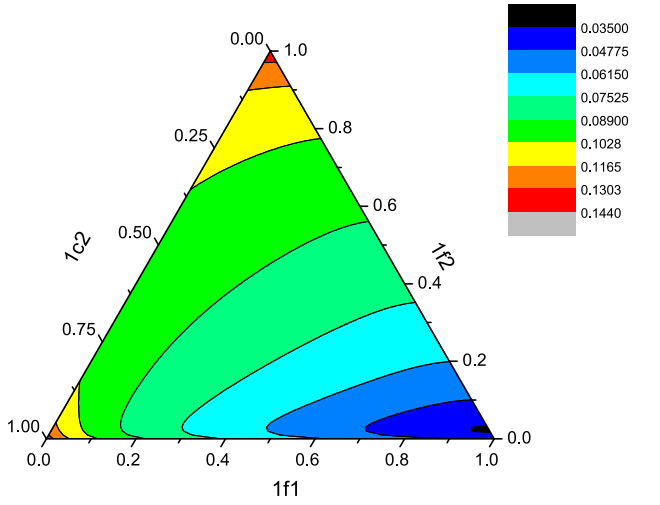

Fig. 12. Conformational analysis of **1** using all our distances. The quality factor q (Eq. (4)) is color-coded. The lower the quality factor, the better the agreement of all experimental distances to the distances averaged from conformers **1f1**, **1f2** and **1c2** by Eq. (1), with the black area being the area of the best agreement. Only if **1f2** is added, an improvement can be observed; no improvement can be found when adding **1c2**. The minimum is at 98% **1f1**, 2% **1f2** and 0%**1c2**.

There are several RDC datasets for strychnine [46,32,47,33,34]. All of them include the RDC C_{12}–H_{12}, the spatial relationship of which changes with respect to the rest of the molecule when adding the conformer **1f2**. The spatial relationships that change the most with respect to the rest of the molecule and therefore are of greatest interest are C_{23}–H_{23a} and C_{23}–H_{23b}. These RDCs are only included in some of the datasets.

The first dataset was published by Thiele et al. [46]. Strychnine was oriented in Poly-γ-benzyl-l-glutamate (PBLG)/$CDCl_3$. The dataset contains very few RDCs, each with large errors, and does not include RDCs for C_{23}–H_{23a} and C_{23}–H_{23b}. Little improvement of the fit is thus expected when adding the second conformer **1f2**. This small improvement is observed (see Fig. 13), which seems to be too small to be of significance.

Next, strychnine was oriented in Poly-γ-ethyl-l-glutamate (PELG)/$CDCl_3$, again by Thiele [32]. This dataset includes RDCs for C_{23}–H_{23a} and C_{23}–H_{23b}. As discussed by Schmidt et al. [27], the

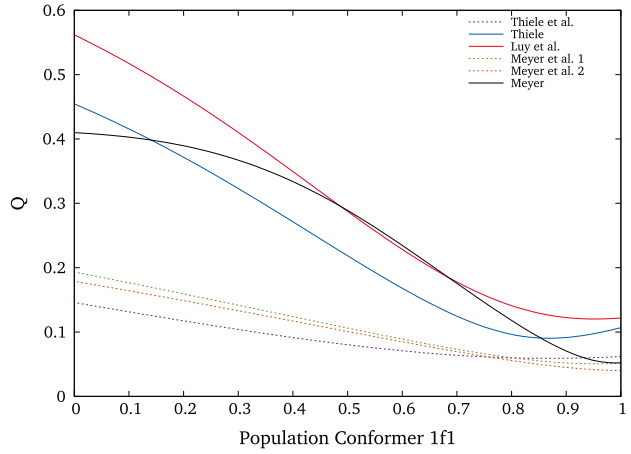

Fig. 13. MCST fits using previously published RDC data for **1** from Thiele et al. [46], Thiele [32], Luy et al. [47], Meyer et al. [33] and Meyer [34]. The solid lines indicate fits that include RDCs for C_{23}–H_{23a} and C_{23}–H_{23b}, while fits represented by the dashed lines do not include these RDCs.

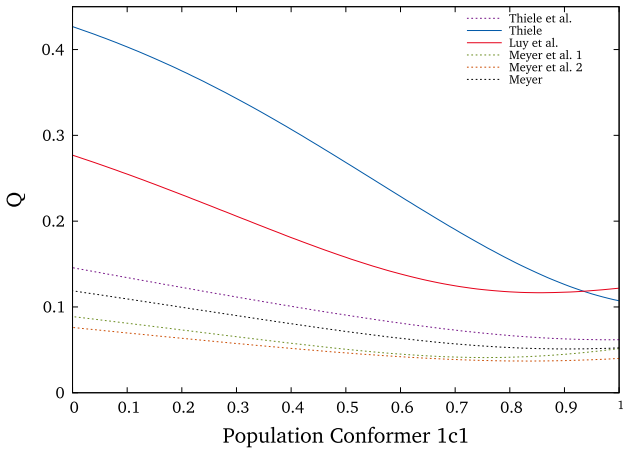

Fig. 14. MCST fits using previously published RDC data for **1** from Thiele et al. [46], Thiele [32], Luy et al. [47], Meyer et al. [33] and Meyer [34]. The solid lines indicate fits that include RDCs in the flexible ring C, while fits represented by the dashed lines do not include these RDCs.

quality of the fit improves when adding a second conformer **1f2**. The best agreement of experimental and calculated RDC data can be found at a population of 87% **1f1**.

RDC data by Luy et al. were measured in cross-linked polystyrene swollen in $CDCl_3$ [47]. This dataset also includes RDCs for C_{23}–H_{23a} and C_{23}–H_{23b}. There is a small improvement of the fit, but it is too small to be of significance.

Meyer et al. recently published two RDC datasets for strychnine aligned in two enantiomers of polyacetylene/$CDCl_3$ [33]. Both datasets do not include RDCs for C_{23}–H_{23a} and C_{23}–H_{23b}, correspondingly the improvement of the fits is small or nonexistent. Another set of RDCs exists from Meyer which includes the RDC for C_{23}–H_{23a} and C_{23}–H_{23b} [34]. The fit shows an improvement when adding **1f2**, but the improvement again is too small to be of significance.

Thus there are data sets (by Thiele [32] and Luy et al. [47]), which show an improvement of the fit when a second conformer is added, but these data sets show the worst overall agreement of experimental and back-calculated RDCs and need to be viewed with caution. The other, newer datasets show no or insignificant improvement when adding **1f2**. In consequence, for strychnine, the RDC analysis is not able to detect a small addition of the second conformer **1f2**. In this particular case, the NOE analysis seems to be superior to the RDC analysis.

Although a flexibility of ring C was not found in the NOE analysis, we chose to investigate this matter further using the RDC datasets. The RDC analysis reveals the same trend as the NOE analysis (see Fig. 14). Only the RDC dataset from Luy et al. [47] shows an improvement when adding a second conformer **1c2**. This improvement is small, and it does not lead to a good description of the system. In accordance with the results of the NOE analysis, the flexibility of ring C is not necessary to describe the experimental data.

A three-conformer-analysis of the RDC data is shown in Supporting Information and leads to the same results as the separate analysis of the rings C and F: Only the RDC dataset from Luy et al. [47] shows a small improvement when adding both **1f2** and **1c2**. The dataset from Thiele [32] only improves when adding **1f2**; adding **1c2** does not improve the quality of the fit.

While one could be tempted to view these small improvements as indicative for a second conformer, we believe that all improvements are too small to be of significance.

4. α-Methylene-γ-butyrolactone 2

The description of dipolar couplings in the presence of conformational flexibility has been extensively studied [48–51,16–18,52–59]. RDCs especially have shown their potential in determining conformer populations [6,5,9,60–64,20,65]. Recently, RDC data has yielded information on both the configuration and conformation of the organic molecule α-methylene-γ-butyrolactone **2**. The goal of the RDC analysis [66] was to determine the relative configuration of the stereogenic centers C_2 and C_3 in the five-membered ring, which was ultimately shown to be *trans*. In addition, it was later shown [19,67] that there are two conformers for the *trans*-configured ring. Using the MCST model, the population of conformer **2trans1** was determined to be (60 ± 20)%. From the (MCMT) model, the extracted population was (65 ± 7)%. These values are in very good agreement with those extracted from *J* coupling constants ((60 ± 20)%). The populations of **2trans1** and **2trans2** (see Fig. 15) were thus determined to be approximately 60% and 40% [19].

Due to the lack of analyte of sufficient purity at that time, it had not been possible to determine significant distances using the NOE [66]. Therefore a determination of the configuration and conformer populations using NOE derived distances could not be achieved. Thus, it was not possible to check whether a conformational analysis using NOE data would lead to the same results as the analysis of the RDC data.

In the meantime, more analyte has been synthesized [68] and purified, enabling us to do a thorough NOE analysis. The distance of greatest interest is the one between the protons H_2 and H_3, which may be *syn* (*cis*-configuration) or *anti* (*trans*-configuration). The resulting experimental distance is closer to the distance corresponding to a *trans* configuration, but significantly deviates from the one expected from the structures (see Fig. 16). In this case, it is not sufficient to look at just one distance, so we performed a full NOE analysis using mixing time series (50–400 ms) of fully relaxed 1D PFGSE NOE spectra with ZQS. As calibration distance, we chose H_{6b}–H_{6a} as rigid distance and set it to 1.886 Å.

We have been able to determine four distances with good precision. Two of those distances include a methyl group. The protons in these groups are assumed to be in the slow tumbling regime [3,12,13]. Therefore, the distances from each of the three methyl protons to the proton showing the NOE are averaged for every conformer according to Tropp [12], using Eq. (2) (r^{-3} averaging).

This averaged methyl distance is then used as $r_{IS,\mu}$ in Eq. (1). This two-step averaging process for methyl groups again has been implemented in *WEEDHEAD*. The result of this analysis is shown in Fig. 17 and demonstrates that the original assignment of *trans* is correct, and leads to conformer populations of 71% **2trans1** and 29% **2trans2**. This is in very good agreement with the RDC data and also with conformer populations approximated from free energy differences in quantum chemical calculations [66,19].

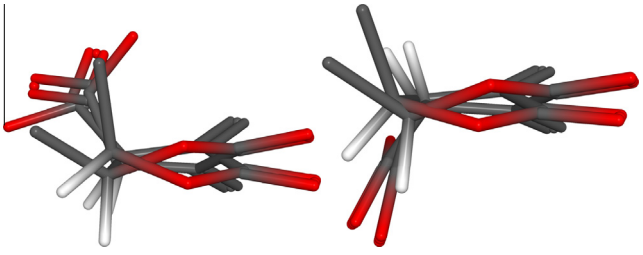

Fig. 15. The two conformers **2cis1** and **2cis2** for the *cis*-configuration (left) and **2trans1** and **2trans2** for the *trans*-configuration (right) of α-methylene-γ-butyrolactone **2** [19].

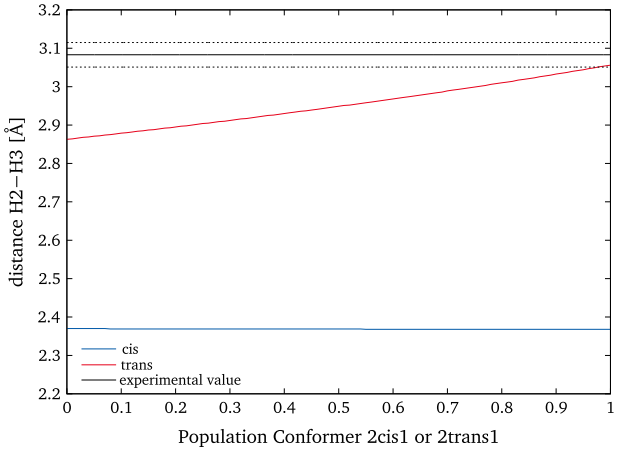

Fig. 16. A comparison of the distance H_2–H_3 in **2** averaged for the *cis*- (blue) and *trans*-configuration (red), respectively, and the experimental value (black, experimental error represented as dashed lines). The experimental distance is too large for both the *cis*- and the *trans*-configuration. It is closer to the *trans*-configuration, but this result should be met with caution. (For interpretation of the references to color in this figure legend, the reader is referred to the web version of this article.)

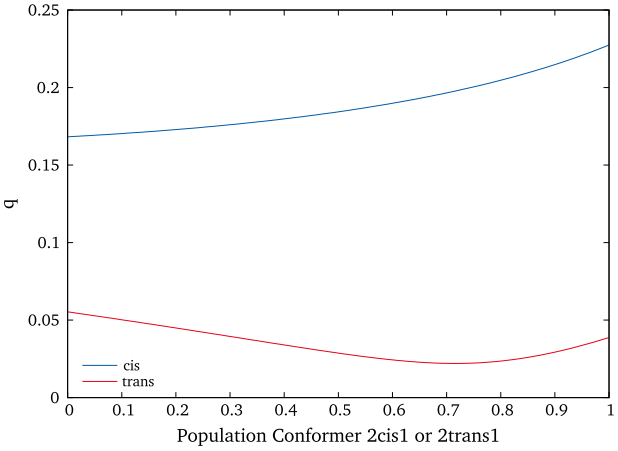

Fig. 17. Conformational analysis of the *cis*- (blue) and the *trans*-configuration (red) of **2**. The quality of the fit is much better for the *trans*-configuration, with a minimum at a population of 71% of **2trans1**. This is in good agreement with the RDC data [66,19]. (For interpretation of the references to color in this figure legend, the reader is referred to the web version of this article.)

It needs to be noted that the experimental value for the distance H_2–H_3 is too large for both the *trans*- and the *cis*-configuration (see Fig. 16). From this, one could assume that the *trans*-configuration seems more reasonable, because the experimental distance is closer to the distance from the *trans*-configuration, but no population information can be extracted. The corresponding PANIC plot (see Supporting Information) shows a rather large scattering of the data points, thus this distance is to be viewed with caution. We believe that in this case it is not sufficient to look at just one distance to determine the relative configuration of the five-membered ring. In this case, the combined NOE/RDC analysis seems to be superior.

For the above analysis, the tumbling has been assumed to be fast. Thus, according to Eq. (1) r^{-6} averaging has been employed. Additionally, we have performed an analysis using r^{-3} averaging according to Eq. (2), which would be correct for slow tumbling. In addition, we have also tried the permutations where the methyl groups are in the fast tumbling regime (r^{-6}), leading to four possible combinations of Eqs. (1) and (2). The best description of the experimental data can be found using the two-step averaging described above (see Supporting Information for details).

5. Conclusion

For strychnine **1**, we confirmed that a second conformer **1f2** has to be taken into account to understand the experimental NOE data. This result is in agreement with the results from Butts et al. [26].

By preparing the sample without oxygen, we excluded paramagnetic relaxation partners. In addition, we excluded possible influences from strong coupling or incomplete relaxation and checked the validity of the initial-rate-approximation. As a result, we were able to determine 33 distances that can only be fully explained when including conformational flexibility at ring F. For this ring, the evaluation of one distance H_{11b}–H_{23b} leads to the same result as an analysis of all 33 distances. Thus for ring F one distance was enough to achieve a correct description of the populations of the conformers.

At ring C, the analysis of only one distance can be misleading. When all distances are taken into account, no improvement can be found when adding a second conformer **1c2**.

In the case of α-methylene-γ-butyrolactone **2**, the evaluation of only one distance leads to the correct assignment of relative configuration, but no populations can be described. It is necessary to evaluate all four accessible distances, leading to populations of 71% **2trans1** and 29% **2trans2**.

The RDC analysis for strychnine **1** only shows weak dependence of the quality factor on conformer populations and thus was not able to detect a second conformer. For α-methylene-γ-butyrolactone **2**, the results of the RDC analysis [66,67,19] match the result from the NOE analysis.

Thus, we believe that both methods have strengths and weaknesses. Due to the r^{-6}-averaging and its local character, the NOE changes significantly if (large) variations over short distances are present, but not if (small) variations in distant parts of the compound are present. The RDC analysis, on the other hand, benefits from its global character, so that changes at distant parts of the compound can be determined, but it will fail if only minor changes in local geometry are present.

In some cases, it can be enough to look at just one of the parameters, or even just one experimental value (as is the case for ring F of strychnine). However, there is no guarantee that this approach will work for a given compound. In our opinion, the best way therefore is to look at both NOE and RDC to benefit from the strengths of both methods.

Acknowledgments

The authors thank Lukas Kaltschnee for the helpful discussions concerning ZQS, Dr. Volker Schmidts for the support in *C* and Dr. Benjamin Böttcher for the supply with α-methylene-γ-butyrolactone **2**.

This work was supported by the European Research Council (ERC starting Grant No. 257041 to C.M.T.) and the EPSRC (Grant EP/H003789/1 to IK).

Appendix A. Supplementary material

Supplementary data associated with this article can be found, in the online version, at http://dx.doi.org/10.1016/j.jmr.2015.10.007.

References

[1] M. Karplus, Contact electron-spin coupling of nuclear magnetic moments, J. Chem. Phys. 30 (1) (1959) 11–15.
[2] I. Solomon, Relaxation processes in a system of two spins, Phys. Rev. 99 (2) (1955) 559–565.
[3] D. Neuhaus, M.P. Williamson, The Nuclear Overhauser Effect in Structural and Conformational Analysis, second ed., Wiley, Chichester, 2000.
[4] B. Vögeli, The nuclear Overhauser effect from a quantitative perspective, Prog. Nucl. Magn. Reson. Spectrosc. 78 (0) (2014) 1–46.
[5] C.M. Thiele, Use of RDCs in rigid organic compounds and some practical considerations concerning alignment media, Concepts Magn. Reson. 30A (2) (2007) 65–80.
[6] C.M. Thiele, Residual dipolar couplings (RDCs) in organic structure determination, Eur. J. Org. Chem. 2008 (34) (2008) 5673–5685.
[7] G. Kummerlöwe, B. Luy, Residual dipolar couplings for the configurational and conformational analysis of organic molecules, Annu. Rep. NMR Spectrosc. 68 (2009) 193–232 (Chapter 4).
[8] R.R. Gil, Constitutional, configurational, and conformational analysis of small organic molecules on the basis of NMR residual dipolar couplings, Angew. Chem. Int. Ed. 50 (32) (2011) 7222–7224.
[9] B. Böttcher, C.M. Thiele, Determining the stereochemistry of molecules from residual dipolar couplings (RDCs), eMagRes, vol. 1, John Wiley & Sons, Ltd., 2012, pp. 169–180.
[10] H. Kessler, Detection of hindered rotation and inversion by NMR spectroscopy, Angew. Chem. Int. Ed. Engl. 9 (6) (1970) 219–235.
[11] C.P. Butts, C.R. Jones, E.C. Towers, J.L. Flynn, L. Appleby, N.J. Barron, Interproton distance determinations by NOE – surprising accuracy and precision in a rigid organic molecule, Org. Biomol. Chem. 9 (1) (2011) 177–184.
[12] J. Tropp, Dipolar relaxation and nuclear Overhauser effects in nonrigid molecules: the effect of fluctuating internuclear distances, J. Chem. Phys. 72 (11) (1980) 6035–6043.
[13] P.F. Yip, D.A. Case, Incorporation of internal motion in NMR refinements based on NOESY data, in: J.C. Hoch, F.M. Poulsen, C. Redfield (Eds.), Computational Aspects of the Study of Biological Macromolecules by Nuclear Magnetic Resonance Spectroscopy, Springer, US, 1991, pp. 317–330.
[14] A. Saupe, Kernresonanzen in kristallinen flüssigkeiten und kristallinflüssigen lösungen. teil 1, Z. Naturforsch. 19a (2) (1964) 161–171.
[15] F. Kramer, M. Deshmukh, H. Kessler, S. Glaser, Residual dipolar coupling constants: an elementary derivation of key equations, Concepts Magn. Reson. 21A (1) (2004) 10–21.
[16] E. Burnell, C. de Lange, On the average orientation of molecules undergoing large-amplitude conformational changes in anisotropic liquids, Chem. Phys. Lett. 76 (2) (1980) 268–272.
[17] E.E. Burnell, C.A. de Lange, O.G. Mouritsen, Effects of intramolecular motion on the magnetic resonance of anisotropic liquids: the equivalence of kinetic and equilibrium statistical mechanical approaches, J. Magn. Reson. 50 (2) (1982) 188–196.
[18] J.W. Emsley, G.R. Luckhurst, C.P. Stockley, A theory of orientational ordering in uniaxial liquid crystals composed of molecules with alkyl chains, Proc. Roy. Soc. Lond. A 381 (1780) (1982) 117–138.
[19] C.M. Thiele, V. Schmidts, B. Böttcher, I. Louzao, R. Berger, A. Maliniak, B. Stevensson, On the treatment of conformational flexibility when using residual dipolar couplings for structure determination, Angew. Chem. Int. Ed. 48 (36) (2009) 6708–6712.
[20] H. Sun, U.M. Reinscheid, E.L. Whitson, E.J. d'Auvergne, C.M. Ireland, A. Navarro-Vázquez, C. Griesinger, Challenge of large-scale motion for residual dipolar coupling based analysis of configuration: the case of fibrosterol sulfate a, J. Am. Chem. Soc. 133 (37) (2011) 14629–14636.
[21] R.B. Woodward, M.P. Cava, W.D. Ollis, A. Hunger, H.U. Daeniker, K. Schenker, The total synthesis of strychnine, J. Am. Chem. Soc. 76 (18) (1954) 4749–4751.
[22] J. Bonjoch, D. Solé, Synthesis of strychnine, Chem. Rev. 100 (9) (2000) 3455–3482.
[23] J.S. Cannon, L.E. Overman, Is there no end to the total syntheses of strychnine? Lessons learned in strategy and tactics in total synthesis, Angew. Chem. Int. Ed. 51 (18) (2012) 4288–4311.
[24] S. Berger, D. Sicker, Classics in Spectroscopy: Isolation and Structure Elucidation of Natural Products, first ed., Wiley-VCH Verlag GmbH & Co. KGaA, Weinheim, 2009.
[25] G. Bifulco, R. Riccio, G.E. Martin, A.V. Buevich, R.T. Williamson, Quantum chemical calculations of $^1J_{CC}$ coupling constants for the stereochemical determination of organic compounds, Org. Lett. 15 (3) (2013) 654–657.
[26] C.P. Butts, C.R. Jones, J.N. Harvey, High precision NOEs as a probe for low level conformers – a second conformation of strychnine, Chem. Commun. 47 (4) (2011) 1193–1195.
[27] M. Schmidt, F. Reinscheid, H. Sun, H. Abromeit, G.K.E. Scriba, F.D. Sönnichsen, M. John, U.M. Reinscheid, Hidden flexibility of strychnine, Eur. J. Org. Chem. 2014 (6) (2014) 1147–1150.
[28] A. Kumar, G. Wagner, R.R. Ernst, K. Wüthrich, Buildup rates of the nuclear Overhauser effect measured by two-dimensional proton magnetic resonance spectroscopy: implications for studies of protein conformation, J. Am. Chem. Soc. 103 (13) (1981) 3654–3658.
[29] M.J. Thrippleton, J. Keeler, Elimination of zero-quantum interference in two-dimensional NMR spectra, Angew. Chem. Int. Ed. 42 (33) (2003) 3938–3941.
[30] K.E. Cano, M.J. Thrippleton, J. Keeler, A. Shaka, Cascaded *z*-filters for efficient single-scan suppression of zero-quantum coherence, J. Magn. Reson. 167 (2) (2004) 291–297.
[31] M.J. Thrippleton, R.A.E. Edden, J. Keeler, Suppression of strong coupling artefacts in J-spectra, J. Mag. Reson. 174 (1) (2005) 97–109.

[32] C.M. Thiele, Simultaneous assignment of all diastereotopic protons in strychnine using RDCs: PELG as alignment medium for organic molecules, J. Org. Chem. 69 (22) (2004) 7403–7413.
[33] N.-C. Meyer, A. Krupp, V. Schmidts, C.M. Thiele, M. Reggelin, Polyacetylenes as enantiodifferentiating alignment media, Angew. Chem. Int. Ed. 51 (33) (2012) 8334–8338.
[34] N. Meyer, Helikal chirale Polyacetylene in Katalyse und Analytik, Ph.D. Thesis, TU Darmstadt, 2012.
[35] J. Stonehouse, P. Adell, J. Keeler, A.J. Shaka, Ultrahigh-quality NOE spectra, J. Am. Chem. Soc. 116 (13) (1994) 6037–6038.
[36] K. Stott, J. Stonehouse, J. Keeler, T.-L. Hwang, A.J. Shaka, Excitation sculpting in high-resolution nuclear magnetic resonance spectroscopy: application to selective NOE experiments, J. Am. Chem. Soc. 117 (14) (1995) 4199–4200.
[37] K. Stott, J. Keeler, Q.N. Van, A.J. Shaka, One-dimensional NOE experiments using pulsed field gradients, J. Magn. Reson. 125 (2) (1997) 302–324.
[38] H. Hu, K. Krishnamurthy, Revisiting the initial rate approximation in kinetic NOE measurements, J. Magn. Reson. 182 (1) (2006) 173–177.
[39] G. Cornilescu, J.L. Marquardt, M. Ottiger, A. Bax, Validation of protein structure from anisotropic carbonyl chemical shifts in a dilute liquid crystalline phase, J. Am. Chem. Soc. 120 (27) (1998) 6836–6837.
[40] S. Macura, B.T. Farmer II, L.R. Brown, An improved method for the determination of cross-relaxation rates from NOE data, J. Magn. Reson. 70 (3) (1986) 493–499.
[41] Spinach version 1.3.1980. <http://spindynamics.org/Spinach.php>.
[42] H.J. Hogben, M. Krzystyniak, G.T.P. Charnock, P. Hore, I. Kuprov, Spinach – a software library for simulation of spin dynamics in large spin systems, J. Magn. Reson. 208 (2) (2011) 179–194.
[43] I. Kuprov, Diagonalization-free implementation of spin relaxation theory for large spin systems, J. Magn. Reson. 209 (1) (2011) 31–38.
[44] A. Karabanov, I. Kuprov, G.T.P. Charnock, A. van der Drift, L.J. Edwards, W. Köckenberger, On the accuracy of the state space restriction approximation for spin dynamics simulations, J. Chem. Phys. 135 (8) (2011) 084106.
[45] V. Schmidts, Entwicklung einer Auswertungssoftware zur Anwendung Residualer Dipolarer Kopplungen in der organischen Strukturaufklärung, Ph. D. Thesis, TU Darmstadt, 2013.
[46] C.M. Thiele, S. Berger, Probing the diastereotopicity of methylene protons in strychnine using residual dipolar couplings, Org. Lett. 5 (5) (2003) 705–708.
[47] B. Luy, K. Kobzar, H. Kessler, An easy and scalable method for the partial alignment of organic molecules for measuring residual dipolar couplings, Angew. Chem. Int. Ed. 43 (9) (2004) 1092–1094.
[48] J.W. Emsley, Liquid crystalline samples: structure of nonrigid molecules, in: Encyclopedia of Magnetic Resonance, John Wiley & Sons, Ltd., 2007.
[49] S. Marčelja, Chain ordering in liquid crystals. I. Even-odd effect, J. Chem. Phys. 60 (9) (1974) 3599–3604.
[50] J.W. Emsley, G.R. Luckhurst, The effect of internal motion on the orientational order parameters for liquid crystalline systems, Mol. Phys. 41 (1) (1980) 19–29.
[51] E.E. Burnell, C.A. de Lange, Effects of interaction between molecular internal motion and reorientation on NMR of anisotropic liquids, J. Magn. Reson. 39 (3) (1980) 461–480.
[52] S. Sinton, D. Zax, J. Murdoch, A. Pines, Multiple-quantum NMR study of molecular structure and ordering in a liquid crystal, Mol. Phys. 53 (2) (1984) 333–362.
[53] C. Zannoni, An internal order parameter formalism for non-rigid molecules, Nuclear Magnetic Resonance of Liquid Crystals, vol. 141, Springer, Netherlands, 1985, pp. 35–52.
[54] J. Emsley, N. Heaton, M. Kimmings, M. Longeri, The conformation and orientational order of 1-ethoxy-4-chlorobenzene dissolved in a nematic liquid crystal, Mol. Phys. 61 (2) (1987) 433–442.
[55] D.J. Photinos, E.T. Samulski, H. Toriumi, Alkyl chains in a nematic field. 1. A treatment of conformer shape, J. Phys. Chem. 94 (11) (1990) 4688–4694.
[56] D. Catalano, L. Di Bari, C.A. Veracini, G.N. Shilstone, C. Zannoni, A maximum-entropy analysis of the problem of the rotameric distribution for substituted biphenyls studied by ^{1}H nuclear magnetic resonance spectroscopy in nematic liquid crystals, J. Chem. Phys. 94 (5) (1991) 3928–3935.
[57] A. Ferrarini, G. Moro, P. Nordio, G. Luckhurst, A shape model for molecular ordering in nematics, Mol. Phys. 77 (1) (1992) 1–15.
[58] R. Berardi, F. Spinozzi, C. Zannoni, Maximum entropy internal order approach to the study of intramolecular rotations in liquid crystals, J. Chem. Soc., Faraday Trans. 88 (1992) 1863–1873.
[59] B. Stevensson, D. Sandström, A. Maliniak, Conformational distribution functions extracted from residual dipolar couplings: a hybrid model based on maximum entropy and molecular field theory, J. Chem. Phys. 119 (5) (2003) 2738–2746.
[60] A. Schuetz, J. Junker, A. Leonov, O.F. Lange, T.F. Molinski, C. Griesinger, Stereochemistry of sagittamide a from residual dipolar coupling enhanced NMR, J. Am. Chem. Soc. 129 (49) (2007) 15114–15115.
[61] C. Farès, J. Hassfeld, D. Menche, T. Carlomagno, Simultaneous determination of the conformation and relative configuration of archazolide a by using nuclear overhauser effects, J couplings, and residual dipolar couplings, Angew. Chem. Int. Ed. 47 (20) (2008) 3722–3726.
[62] R.S. Stoll, M.V. Peters, A. Kuhn, S. Heiles, R. Goddard, M. Bühl, C.M. Thiele, S. Hecht, Photoswitchable catalysts: correlating structure and conformational dynamics with reactivity by a combined experimental and computational approach, J. Am. Chem. Soc. 131 (1) (2009) 357–367.
[63] B. Böttcher, V. Schmidts, J.A. Raskatov, C.M. Thiele, Determination of the conformation of the key intermediate in an enantioselective palladium-catalyzed allylic substitution from residual dipolar couplings, Angew. Chem. Int. Ed. 49 (1) (2010) 205–209.
[64] P. Trigo-Mouriño, R. Santamaría-Fernández, V.M. Sánchez-Pedregal, A. Navarro-Vázquez, Conformational analysis of an isoquinolinium hydrochloride in water using residual dipolar couplings, J. Org. Chem. 75 (9) (2010) 3101–3104.
[65] V. Schmidts, M. Fredersdorf, T. Lübken, A. Porzel, N. Arnold, L. Wessjohann, C. M. Thiele, RDC-based determination of the relative configuration of the fungicidal cyclopentenone 4,6-diacetylhygrophorone A^{12}, J. Nat. Prod. 76 (5) (2013) 839–844.
[66] C.M. Thiele, A. Marx, R. Berger, J. Fischer, M. Biel, A. Giannis, Determination of the relative configuration of a five-membered lactone from residual dipolar couplings, Angew. Chem. Int. Ed. 45 (27) (2006) 4455–4460.
[67] C.M. Thiele, A. Maliniak, B. Stevensson, Use of local alignment tensors for the determination of relative configurations in organic compounds, J. Am. Chem. Soc. 131 (36) (2009) 12878–12879.
[68] M. Biel, A. Kretsovali, E. Karatzali, J. Papamatheakis, A. Giannis, Design, synthesis, and biological evaluation of a small-molecule inhibitor of the histone acetyltransferase Gcn5, Angew. Chem. Int. Ed. 43 (30) (2004) 3974–3976.